^{13}C and ^{1}H spectra were run in 10-mm tubes.

The isotropic shifts (low-field shifts negative) were obtained by measuring the shift relative solvent signals (benzene, ^{1}H δ 7.3; toluene, $C^{1}H_3$ δ 2.3, $^{13}CH_3$ δ 20.3; THF, ^{13}C-β δ 26.0) and calculating it relative to the signal of a similar diamagnetic compound. For the bent vanadocene units ferrocene signals were taken ($(C_5H_5)_2Fe$, ^{1}H δ 4.1, ^{13}C δ 67.8; $(CH_3C_5H_4)_2Fe$, $C_5{}^{1}H_4$ δ 4.0, $C^{1}H_3$ δ 1.8 and ref 18; $(C_5Me_4Et)_2Fe$, cf. ref 9 and 19) while the aromatic signals of *p*-diethynylbenzene (^{1}H δ 7.4; $^{13}C1/4$ δ ~120, $^{13}C2,3,5,6$ δ ~128 analogous to ref 20) and benzene were chosen as standard signals for the bridge protons.

The variable-temperature results were subjected to a least-squares fit analysis which also gave the data of Table II except **9** where the 298 K shifts were calculated with the assumption of an unimportant deviation from the Curie law. Digital accuracy for ^{1}H and ^{13}C was 0.17 and 0.35 ppm, respectively.

Crystal Measurements. Cell dimensions were obtained on a Syntex $P2_1$ four-circle diffractometer by centering and subsequent refinement of 15 high-angle reflections from different parts of the reciprocal space at room temperature: a = 607.9 (4), b = 1755.5 (9), c = 2277.2 (15) pm. The space group $P2_12_12_1$ was inferred from systematic extinctions. With Z = 4, the calculated density is 1.35 g/cm^3. Intensity measurements were collected between $2° \le 2\theta \le 48°$ (2212 independent reflections) with use of Mo Kα radiation (λ = 71.069 pm, graphite monochromator). After Lorentz and polarization corrections (no absorption correction, μ = 8.3 cm^{-1}), 1660 structure factors ($F_o \ge 3.92\sigma(F_o)$) were obtained.

Solution and Refinement of the Structure. The positions of the vanadium atoms were located by a Patterson function. Subsequent difference Fourier maps revealed the positions of all carbon atoms and some of the hydrogen atoms. The positions of the remaining hydrogen atoms were calculated according to ideal geometry. Refinement by the full-matrix least-squares method using anisotropic thermal parameters for the metal atoms and some of the carbon atoms converged to R_1 = 0.077 and R_2 = 0.074. The hydrogen parameters were not refined. The final atomic parameters are given in Table IV.

Acknowledgment. We are grateful to the Deutsche Forschungsgemeinschaft and the Fonds der Chemischen Industrie which supported our studies in part.

Registry No. **5**, 79102-48-0; **9**, 79121-07-6; **10**, 79152-69-5; bromo(ethyltetramethyl-η^5-cyclopentadienyl)vanadium, 68185-51-3; $(C_5H_5)_2VCl$, 12701-79-0; $(C_5H_4Me)_2VCl$, 66446-72-8; **12**, 12212-56-5.

Supplementary Material Available: A listing of structure factors (10 pages). Ordering information is given on any current masthead page.

(18) Köhler, F. H.; Matsubayashi, G. *J. Organomet. Chem.* **1975**, *96*, 391–397.
(19) Feitler, D.; Whitesides, G. M. *Inorg. Chem.* **1976**, *15*, 466–468.
(20) Formáček, V.; Desnoyer, L.; Kellerhals, H. P.; Keller, T.; Clerc, J. T. "^{13}C Data Bank"; Bruker-Physik: Karlsruhe, 1976; Vol. 1, pp 46, 47.

Contribution from the Department of Chemistry, University of Minnesota, Minneapolis, Minnesota 55455

Rhodium Complexes of 1,4-Bis(diphenylphosphino)butane. Crystal and Molecular Structures of $[Rh(dppb)_2]BF_4 \cdot C_4H_{10}O$ and $[Rh(cod)(dppb)]BF_4$

MICHAEL P. ANDERSON and LOUIS H. PIGNOLET*

Received June 15, 1981

Bis(diphosphine) complexes of Rh(I) of the type $[Rh(Ph_2P(CH_2)_nPPh_2)_2]BF_4$ where n = 3 and 4 have been examined by using low-temperature ^{31}P NMR spectroscopy and found to have complex solution geometries. For n = 3 the solution geometry (solvent = acetone) is trigonal bipyramidal with an equatorial solvent molecule as evidenced by an A_2B_2X $^{31}P\{^{1}H\}$ NMR spectrum at −80 °C. For n = 4 the solution geometry is more complex and probably involves dppb-bridged solvated species. Single-crystal X-ray structures were determined for the n = 4 complex, $[Rh(dppb)_2]BF_4 \cdot C_4H_{10}O$, and for $[Rh(cod)(dppb)]BF_4$, where cod is 1,5-cyclooctadiene. Both complexes crystallize in the monoclinic space group $C2/c$. The former has unit cell parameters a = 36.60 (1) Å, b = 14.248 (8) Å, c = 26.220 (4) Å, and β = 125.18 (2)°, and for the latter a = 30.59 (1) Å, b = 10.326 (1) Å, c = 25.044 (8) Å, and β = 123.36 (2)°. $[Rh(dppb)_2]^+$ possesses a coordination core geometry which is significantly distorted toward tetrahedral whereas $[Rh(cod)(dppb)]^+$ has an approximately square-planar geometry. The distortion in the former complex results from phosphine–phosphine repulsions. These repulsions also cause a significant lengthening in one of the Rh–P bonds [2.361 (2) Å] compared with the average value for the other three [2.318 (2) Å]. This bond weakening is presumably responsible for the propensity of this complex to form dppb-bridged dimeric species.

Introduction

Considerable interest has recently been focused on cationic rhodium(I) complexes containing chelating diphosphine ligands, particularly with respect to their use in catalytic hydrogenation[1-4] and decarbonylation[5,6] reactions. Of special importance has been the successful inducement of optical activity by hydrogenation of prochiral olefins using cationic rhodium complexes with chiral diphosphine ligands.[1-4,7] During the course of our studies on catalytic decarbonylation reactions[5,6,8] using $Rh[(Ph_2P(CH_2)_nPPh_2]_2^+$ complexes, **1**, with n = 1–4, it became increasingly obvious that the nature of these species in solution was not well understood. For example, the low-temperature $^{31}P\{^{1}H\}$ NMR spectra of $[Rh(dppp)_2]BF_4$ (**1**, n = 3) and $[Rh(dppb)_2]BF_4$ (**1**, n = 4) showed complex patterns that are inconsistent with simple square-planar coordination (vide infra).[5] In view of the importance of these complexes, we report here the results of a variable-temperature ^{31}P NMR study on complexes **1**, n = 3 and 4, and of single-crystal X-ray characterizations of $[Rh(dppb)_2]BF_4$ (**1**, n = 4) and $[Rh(cod)(dppb)]BF_4$ (**2**), where cod = 1,5-cyclooctadiene. With the exception of a brief abstract,[9] this is only the second[10]

(1) Chan, A. S. C.; Pluth, J. J.; Halpern, J. *J. Am. Chem. Soc.* **1980**, *102*, 5952.
(2) Fryzuk, M. D.; Bosnich, B. *J. Am. Chem. Soc.* **1977**, *99*, 6262.
(3) Knowles, W. S.; Sabacky, M. J.; Vineyard, B. D. *Adv. Chem. Ser.* **1974**, *No. 132*, 274.
(4) James, B. R.; Mahajan, D. *Can. J. Chem.* **1979**, *57*, 180.
(5) Doughty, D. H.; Anderson, M. P.; Casalnuovo, A. L., McGuiggan, M. F.; Tso, C. C.; Wang, H. H.; Pignolet, L. H. *Adv. Chem. Ser.*, in press.
(6) Doughty, D. H.; Pignolet, L. H. *J. Am. Chem. Soc.* **1978**, *100*, 7083.
(7) Brown, J. M.; Chaloner, P. A. *J. Chem. Soc., Chem. Commun.* **1980**, 344.
(8) Doughty, D. H.; McGuiggan, M. F.; Wang, H. H.; Pignolet, L. H. In "Fundamental Research in Homogeneous Catalysis"; Tsutsui, M., Ed.; Plenum Press: New York, 1979; Vol. 3, p 909.
(9) Knowles, W. S. "Abstracts of Papers"; American Crystallographic Association: 1978; Vol. 6, No. PA1.

0020-1669/81/1320-4101$01.25/0

reported single-crystal X-ray characterization of dppb metal complexes of which we are aware.

Experimental Section

Reagents and Solvents. Rhodium trichloride hydrate was obtained from Matthey Bishop, Inc. 1,4-Bis(diphenylphosphino)butane (dppb) and 1,3-bis(diphenylphosphino)propane (dppp) were purchased from Strem Chemicals and used without further purification. All solvents were reagent grade. 1,5-Cyclooctadiene was purchased from Aldrich Chemical Co. and was used without purification.

Physical Measurements. ^{31}P NMR spectra were recorded at 40.5 MHz by using a Varian Associates XL-100 FT instrument, and chemical shifts were referenced to external standard H_3PO_4 with positive shifts downfield. Analytical data were determined by Galbraith Laboratories.

Preparation of Compounds. $[Rh(dppb)_2]BF_4 \cdot C_4H_{10}O$ (1, $n = 4$). All steps were carried out under a purified N_2 atmosphere by using standard Schlenk techniques. An acetone solution of $AgBF_4$ (0.165 g, 0.848 mmol) was added to a slurry of $[Rh(cod)Cl]_2$[11] (0.201 g, 0.814 mmol Rh) in acetone. The resulting mixture, which contained AgCl(s), was refluxed for 30 min and filtered. The yellow filtrate solution was added to a 2-fold excess of dppb (0.836 g, 1.96 mmol) dissolved in toluene, resulting in a dark burgundy solution. Upon removal of the acetone during reflux, a deep red precipitate of $[Rh(dppb)_2]BF_4$ formed. The precipitate was filtered and washed with ether. Recrystallization by solvent diffusion using CH_2Cl_2 and $C_4H_{10}O$ yielded large red crystals of the product as an ether solvate in 84% yield. ^{31}P NMR (CH_2Cl_2): δ 20.6 (d, J_{Rh-P} = 136 Hz). Anal. Calcd for $RhC_{60}H_{66}P_4BF_4$: C, 64.53; H, 5.96. Found: C, 64.65; H, 5.58.

$[Rh(cod)(dppb)]BF_4$ (2) was obtained as orange crystals by the same method but by using a 1:1 mole ratio of Rh to dppb. ^{31}P NMR (CH_2Cl_2): δ = 23.51 (d, J_{Rh-P} = 144 Hz). Anal. Calcd for $RhC_{36}H_{40}P_2BF_4$: C, 59.69; H, 5.57. Found: C, 59.78; H, 5.61.

$[Rh(dppp)_2]BF_4$ (1, $n = 3$) was prepared as previously described.[6]

Collection and Reduction of X-ray Data. A summary of crystal data is presented in Table I. Crystals of **1**, $n = 4$, and **2** were secured to the end of glass fibers with 5-min epoxy resin. The crystals were found to belong to the *C*-centered monoclinic crystal class by the Enraf-Nonius CAD 4-SDP peak search, centering, and indexing programs and by a Delaunay reduction calculation (program tracer).[12] The space group $C2/c$ was chosen from the systematic absences observed during data collection (vide infra) (hkl, $h + k = 2n + 1$; $h0l$, $l = 2n + 1$) and was verified by successful solution and refinement (vide infra). Data collections were carried out on a CAD 4 Nonius diffractometer. Background counts were measured at both ends of the scan range with the use of an ω–2θ scan, equal, at each side, to one-fourth of the scan range of the peak. In this manner, the total duration of background measurements is equal to half of the time required for the peak scan. The intensities of three standard reflections were measured every 1.5 h of X-ray exposure for both **1**, $n = 4$, and **2**, and no decay with time was noted. The data were corrected for Lorentz, polarization, and background effects.

Solution and Refinement of the Structures. Both structures were solved by conventional heavy-atom techniques. The Rh atoms were located by Patterson syntheses. Full-matrix least-squares refinement and difference-Fourier calculations were used to locate all remaining nonhydrogen atoms. The atomic scattering factors were taken from the usual tabulation,[13] and the effects of anomalous dispersion were included in F_c by using Cromer and Ibers[14] values of $\Delta f'$ and $\Delta f''$. Two tables of observed and calculated structure factor amplitudes for **1**, $n = 4$, and **2** are available.[15] For **1**, $n = 4$, an ether solvate molecule was located by difference-Fourier analysis and was refined, giving large thermal parameters. The presence of the solvate was confirmed by ^1H NMR. Due to disorder in this solvate molecule, atom CS2 was fixed in the last least-squares cycles in a chemically reasonable position. The final difference-Fourier map did not reveal significant residual electron density in this region. The Rh, P, and F atoms in **1**, $n = 4$, were refined with anisotropic thermal parameters while all other nonhydrogen atoms were refined isotropically. Hydrogen atom positions were not included. The largest peak in the final difference-Fourier map was 0.3 e/Å^3 and was located near the BF_4 group. For **2**, all nonhydrogen atoms were refined thermally anisotropically. Hydrogen atom positions were calculated (C–H distance set at 0.95 Å) and included in structure factor calculations but were not refined. The largest peak in the final difference-Fourier map was 0.4 e/Å^3 and was located near the BF_4 group. The final positional and thermal parameters of the atoms appear in Tables II and III and as supplementary material.[15] The labeling schemes for **1**, $n = 4$, and **2** are presented in Figures 1 and 2, respectively. In **2**, hydrogen atoms are labeled the same as the carbon atoms to which they are attached.

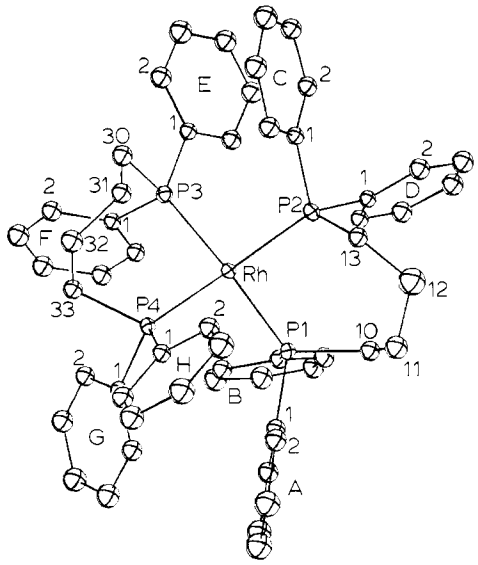

Figure 1. ORTEP drawing of the cation $[Rh(dppb)_2]^+$ showing the labeling scheme (30% probability ellipsoids).

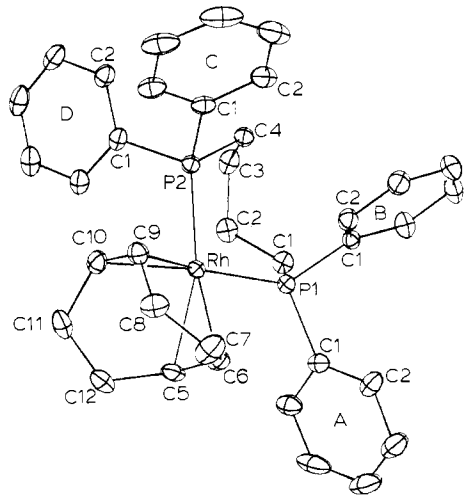

Figure 2. ORTEP drawing of the cation $[Rh(cod)(dppb)]^+$ showing the labeling scheme (30% probability ellipsoids).

Results and Discussion

^{31}P NMR Results. The room-temperature $^{31}P\{^1H\}$ NMR spectra of $[Rh(dppp)_2]BF_4$ (**1**, $n = 3$) and $[Rh(dppb)_2]BF_4$ (**1**, $n = 4$), recorded with use of acetone as solvent, show simple

(10) Pignolet, L. H.; Doughty, D. H.; Nowicki, S. C.; Anderson, M. P.; Casalnuovo, A. L. *J. Organomet. Chem.* **1980**, *202*, 211.
(11) Chatt, J.; Venanzi, L. M. *J. Chem. Soc.* **1957**, 4735.
(12) All calculations were carried out on PDP 8A and 11/34 computers with use of the Enraf-Nonius CAD 4-SDP programs. This crystallographic computing package is described by: Frenz, B. A. In "Computing in Crystallography"; Schenk, H., Olthof-Hazekamp, R., van Koningsveld, H., Bassi, G. C., Eds.; Delft University Press: Delft, Holland, 1978; pp 64–71; also "CAD 4 and SDP User's Manual"; Enraf-Nonius: Delft, Holland, 1978.
(13) Cromer, D. T.; Waber, J. T. "International Tables for X-ray Crystallography"; Kynoch Press: Birmingham, England, 1974; Vol. IV, Table 2.2.4. Cromer, D. T. *Ibid.*, Table 2.3.1.
(14) Cromer, D. T.; Ibers, J. A. In ref 13.
(15) See paragraph at end of paper regarding supplementary material.

Table I. Summary of Crystal Data and Intensity Collection

	compd 1, $n = 4$	compd 2
	Crystal Parameters	
crystal system	monoclinic	monoclinic
space group	$C2/c$ (No. 15)	$C2/c$ (No. 15)
cell parameters		
a, Å	36.60 (1)	30.69 (1)
b, Å	14.248 (8)	10.326 (1)
c, Å	26.220 (4)	25.044 (8)
β, deg	125.18 (2)	123.36 (2)
V, Å^3	11 177	6629
Z	8	8
calcd density, g/cm^3	1.327	1.452
temp, °C	22	22
abs coeff, cm^{-1}	4.7	6.5
formula	$C_{60}H_{66}BF_4OP_4Rh$	$C_{36}H_{40}BF_4P_2Rh$
fw	1117	724
	Measurement of Intensity Data	
diffractometer	CAD4	CAD4
radiation	Mo K$\bar{\alpha}$ (λ = 0.710 69 Å) graphite monochromatized	Mo K$\bar{\alpha}$ (λ = 0.710 69 Å) graphite monochromatized
scan range, 2θ, deg	0–50	0–48
unique reflctns measd (quadrant)	5170 ($+h,+k,\pm l$)	5186 ($\pm h,-k,+l$)
obsd reflctns[a]	3596 [$F_o^2 \geq 2.5\sigma(F_o^2)$]	3833 [$F_o^2 \geq 2.5\sigma(F_o^2)$]
refinement by full matrix least-squares		
no. of parameters	311	397
R[b]	0.064	0.043
R_w[b]	0.080	0.054
GOF[b]	2.5	1.7
p[a]	0.04	0.04

[a] The intensity data were processed as described in: "CAD4 and SDP User's Manual"; Enraf-Nonius: Delft, Holland, 1978. The net intensity I is given as $I = [K/(\mathrm{NPI})](C - 2B)$, where K = 20.1166 × attenuator factor, NPI = ratio of fastest possible scan rate to scan rate for the measurement, C = total count, and B = total background count. The standard deviation in the net intensity is given by $[\sigma(I)]^2 = (K/(\mathrm{NPI}))^2[C + 4B + (pI)^2]$, where p is a factor used to downweight intense reflections. The observed structure factor amplitude F_o is given by $F_o = (I/Lp)^{1/2}$, where Lp = Lorentz and polarization factors. The $\sigma(I)$'s were converted to the estimated errors in the relative structure factors $\sigma(F_o)$ by $\sigma(F_o) = {}^1/_2[\sigma(I)/I]F_o$. [b] The function minimized was $\Sigma w(|F_o| - |F_c|)^2$, where $w = 1/[\sigma(F_o)]^2$. The unweighted and weighted residuals are defined as $R = (\Sigma||F_o| - |F_c||)/\Sigma|F_o|$ and $R_w = [(\Sigma w(|F_o| - |F_c|)^2/(\Sigma w|F_o|)^2]^{1/2}$. The error in an observation of unit weight (GOF) is $[\Sigma w(|F_o| - |F_c|)^2/(\mathrm{NO} - \mathrm{NV})]^{1/2}$, where NO and NV are the number of observations and variables, respectively.

doublet patterns [δ 7.00 (J = 132 Hz) and δ 20.7 (J = 137 Hz), respectively] and are each indicative of four equivalent phosphorus atoms as expected in square-planar coordination. However, when the temperature is lowered, the spectra of both complexes become more complex as is shown in Figures 3 and 4. For **1**, n = 3, a relatively simple A_2B_2X pattern emerges at temperatures below ca. −60 °C, which is typical of five-coordinate pentagonal-bipyramidal geometry with the diphosphine ligands spanning axial and equatorial positions. See, for example, the $^{31}P\{^1H\}$ NMR spectra of $Rh[Ph_2P(CH_2)_nPPh_2]_2CO^+$, where n = 1 and 3.[16,17] This spectrum is therefore consistent with a monosolvated complex with the solvent (acetone) ligand occupying an equatorial position. Evidence for a similar five-coordinated benzaldehyde solvate

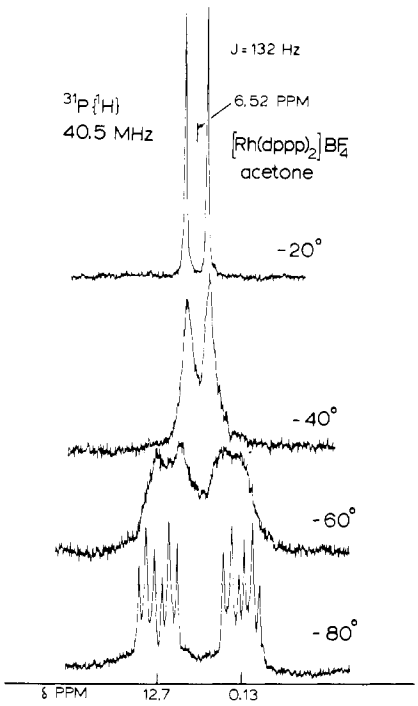

Figure 3. $^{31}P\{^1H\}$ NMR spectra of $[Rh(dppp)_2]BF_4$ recorded with use of acetone solvent.

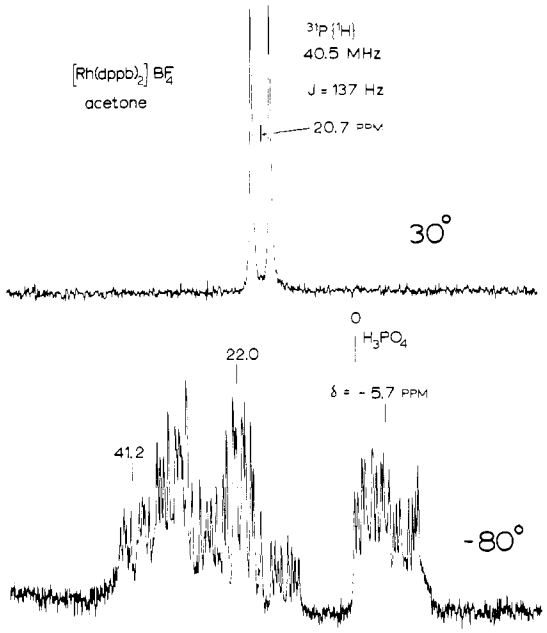

Figure 4. $^{31}P\{^1H\}$ NMR spectra of $[Rh(dppb)_2]BF_4$ recorded with use of acetone solvent.

of $Rh(dppp)_2^+$ has recently been found from kinetic experiments on the catalytic decarbonylation reaction.[5] The coalescence of the A_2B_2X pattern into a doublet is due to stereochemical nonrigidity in $Rh(dppp)_2(acetone)^+$.

A more complicated $^{31}P\{^1H\}$ NMR spectrum is observed for **1**, n = 4, at temperatures below ca. −70 °C (Figure 4). This pattern is very complex and has not been assigned. It presumably results from a combination of solvent association and the presence of dimeric species. It has previously been established that the reaction of CO with **1**, n = 4, at 25 °C in CH_2Cl_2 solution gives several products, one of which is the binuclear compound $[Rh_2(dppb)_3(CO)_4]^{2+}$.[10] The apparent ease with which the dppb ligand dissociates to form bridged binuclear species is probably in part responsible for the complexity of the low-temperature $^{31}P\{^1H\}$ NMR spectrum of **1**,

(16) Pignolet, L. H.; Doughty, D. H.; Nowicki, S. C.; Casalnuovo, A. L. *Inorg. Chem.* **1980**, *19*, 2172.
(17) Sanger, A. R. *J. Chem. Soc., Dalton Trans.* **1977**, 120.

Table II. Positional and Thermal Parameters and Their Estimated Standard Deviations for $[Rh(dppb)_2]BF_4 \cdot C_4H_{10}O$

atom	*x*	*y*	*z*	*B*, Å²	atom	*x*	*y*	*z*	*B*, Å²
Rh1	0.16659 (2)	0.06558 (6)	0.55887 (3)	1.723[a]	C3D	0.1510 (3)	0.2316 (9)	0.7613 (4)	4.8 (3)
P1	0.09117 (7)	0.0493 (2)	0.5175 (1)	2.165[a]	C3E	0.3466 (4)	0.0250 (9)	0.8042 (5)	5.6 (3)
P2	0.17475 (8)	0.1779 (2)	0.6280 (1)	1.843[a]	C3F	0.2716 (3)	−0.2450 (9)	0.5846 (4)	5.0 (3)
P3	0.24137 (8)	0.0209 (2)	0.6172 (1)	1.937[a]	C3G	0.1282 (3)	−0.2517 (9)	0.4160 (4)	4.8 (3)
P4	0.16012 (7)	0.0247 (2)	0.4667 (1)	1.825[a]	C3H	0.1231 (4)	0.2881 (9)	0.3907 (5)	5.8 (3)
F1	0.1302 (4)	−0.4236 (8)	0.5098 (4)	6.962[a]	C4A	−0.0225 (4)	0.0279 (10)	0.3071 (5)	6.4 (3)
F2	0.1098 (4)	−0.5586 (11)	0.4737 (6)	10.559[a]	C4B	0.0784 (4)	−0.2421 (9)	0.5846 (5)	5.7 (3)
F3	0.1721 (3)	0.4551 (11)	0.5291 (4)	11.159[a]	C4C	0.3152 (3)	0.3162 (9)	0.7414 (5)	5.2 (3)
F4	0.1442 (4)	0.5235 (7)	0.4435 (4)	4.937[a]	C4D	0.1394 (3)	0.1431 (9)	0.7707 (4)	5.0 (3)
C10	0.0613 (3)	0.1285 (8)	0.5390 (4)	3.8 (2)	C4E	0.3252 (3)	0.0113 (9)	0.8319 (5)	5.1 (3)
C11	0.0558 (3)	0.2323 (9)	0.5170 (4)	5.0 (3)	C4F	0.2423 (3)	−0.2992 (9)	0.5874 (4)	4.7 (3)
C12	0.0934 (4)	0.2986 (11)	0.5680 (5)	6.9 (4)	C4G	0.0848 (3)	−0.2473 (9)	0.3605 (5)	5.5 (3)
C13	0.1412 (3)	0.2852 (8)	0.5846 (4)	3.5 (2)	C4H	0.1093 (4)	0.2754 (9)	0.3290 (5)	5.8 (3)
C30	0.2803 (3)	0.0840 (8)	0.6045 (4)	4.0 (2)	C5A	−0.0171 (4)	−0.0424 (9)	0.3453 (5)	5.8 (3)
C31	0.2544 (3)	0.1423 (8)	0.5411 (4)	3.7 (2)	C5B	0.0964 (4)	−0.2336 (9)	0.5492 (5)	5.6 (3)
C32	0.2414 (3)	0.0882 (8)	0.4838 (4)	4.6 (3)	C5C	0.2857 (3)	0.3293 (9)	0.6757 (4)	4.9 (3)
C33	0.2113 (3)	0.0012 (7)	0.4689 (4)	3.4 (2)	C5D	0.1402 (3)	0.0648 (9)	0.7395 (4)	4.7 (3)
C1A	0.0454 (3)	0.0392 (7)	0.4329 (4)	3.5 (2)	C5E	0.2805 (3)	−0.0055 (9)	0.7998 (4)	4.7 (3)
C1B	0.0873 (3)	−0.0624 (8)	0.5471 (4)	3.6 (2)	C5F	0.2137 (3)	−0.2595 (8)	0.6006 (4)	4.4 (3)
C1C	0.2298 (3)	0.2328 (7)	0.6735 (4)	2.8 (2)	C5G	0.0630 (3)	−0.1625 (9)	0.3353 (5)	5.4 (3)
C1D	0.1625 (3)	0.1622 (7)	0.6865 (4)	2.8 (2)	C5H	0.1098 (3)	0.1859 (9)	0.3077 (4)	5.0 (3)
C1E	0.2755 (3)	0.0166 (7)	0.7025 (4)	3.0 (2)	C6A	0.0180 (3)	−0.0385 (8)	0.4112 (4)	4.2 (3)
C1F	0.2442 (3)	−0.1051 (7)	0.6054 (4)	3.0 (2)	C6B	0.1017 (3)	−0.1450 (8)	0.5313 (4)	4.1 (3)
C1G	0.1289 (3)	−0.0807 (7)	0.4223 (4)	3.1 (2)	C6C	0.2431 (3)	0.2852 (8)	0.6416 (4)	4.0 (2)
C1H	0.1383 (3)	0.1218 (7)	0.4114 (4)	3.0 (2)	C6D	0.1519 (3)	0.0763 (7)	0.6970 (4)	3.4 (2)
C2A	0.0405 (3)	0.1110 (8)	0.3947 (4)	4.4 (3)	C6E	0.2546 (3)	−0.0034 (8)	0.7316 (4)	4.0 (3)
C2B	0.0703 (3)	−0.0731 (8)	0.5828 (4)	4.3 (2)	C6F	0.2151 (3)	−0.1623 (8)	0.6096 (4)	3.5 (2)
C2C	0.2586 (3)	0.2245 (8)	0.7388 (4)	3.8 (2)	C6G	0.0848 (3)	−0.0756 (8)	0.3661 (4)	4.0 (2)
C2D	0.1628 (3)	0.2418 (8)	0.7183 (4)	4.3 (3)	C6H	0.1243 (3)	0.1078 (8)	0.3498 (4)	4.0 (2)
C2E	0.3216 (3)	0.0285 (8)	0.7381 (4)	4.5 (3)	CS1	−0.0029 (23)	0.5514 (59)	0.0776 (32)	40.0 (33)
C2F	0.2739 (3)	−0.1455 (8)	0.5938 (4)	4.0 (2)	CS3	0.0336 (15)	0.6765 (40)	0.1715 (19)	32.3 (21)
C2G	0.1502 (3)	−0.1657 (8)	0.4468 (4)	3.7 (2)	CS4	0.0489 (22)	0.5844 (59)	0.1947 (30)	50.0 (35)
C2H	0.1373 (3)	0.2098 (8)	0.4309 (4)	3.9 (2)	O1	0.0100 (11)	0.6714 (28)	0.1136 (14)	24.1 (14)
C3A	0.0039 (4)	0.1056 (10)	0.3277 (5)	6.1 (3)	B	0.1430 (6)	0.507 (2)	0.4886 (8)	8.7 (5)
C3B	0.0657 (3)	−0.1641 (9)	0.6001 (4)	5.0 (3)	CS2[b]	0.0098 (0)	0.500 (0)	0.0254 (0)	40.0 (0)
C3C	0.3013 (3)	0.2645 (8)	0.7718 (4)	4.2 (3)					

[a] Equivalent isotropic *B*'s are reported here; anisotropic thermal parameters are reported in the supplementary material. [b] Atom positional and thermal parameters are not refined in final least-squares analyses due to disorder (see text).

$n = 4$. It is important to note that the resonance positions observed in this spectrum rule out the presence of monodentate coordinated dppb with one end dangling. An uncoordinated phosphorus atom in dppb would resonate at δ −17.3 under similar conditions, and no such peak is present in the low-temperature limiting spectrum. These results demonstrate that complexes **1**, $n = 3$ and 4, do not have simple square-planar coorination in acetone solution. Qualitatively similar variable-temperature ^{31}P NMR spectra have also been observed with CH_2Cl_2 as solvent. This shows that for these complexes a square-planar geometry should not be assumed in the solution phase. In contrast, the low-temperature $^{31}P\{^1H\}$ NMR spectrum of $[Rh(dppe)_2]BF_4$ (**1**, $n = 2$) recorded with use of acetone solvent at −79 °C shows a sharp doublet pattern (δ 57.6, $J = 133$ Hz) indicative of a square-planar geometry.

The $^{31}P\{^1H\}$ NMR spectrum of $[Rh(cod)(dppb)]BF_4$ (**2**) recorded with use of acetone solvent consists of a sharp doublet at 30 °C (δ 23.5, $J = 144$ Hz), which broadens significantly as the temperature is lowered to −80 °C. This broadening, which is indicative of the onset of a slow kinetic process, suggests that **2** also has a solution geometry more complex than square-planar. Similar behavior has been observed with the diop analogue $[Rh(cod)(diop)]^+$ (diop = 2,3-(isopropylidenedioxy)-1,4-bis(diphenylphosphino)butane).[18] Both of these complexes contain seven-membered chelate rings.

In light of the above NMR results it was decided to carry out X-ray structural determinations on **1**, $n = 4$, and **2** in order to examine their solid-state geometries in detail. Prior to this work only one single-crystal X-ray structure has been reported in detail for a dppb–metal complex.[10]

X-ray Structural Results. Single-crystal X-ray structures were determined for $[Rh(dppb)_2]BF_4$ (**1**, $n = 4$) and $[Rh(cod)(dppb)]BF_4$ (**2**). Relevant crystallographic data are given in Table I, and positional and thermal parameters are reported in Tables II and III and as supplementary material.[15] Figures 1 and 2 show ORTEP drawings of the molecular structures of both cations including labeling schemes.

The structure of **1**, $n = 4$, consists of discrete cations, anions, and ether solvate molecules. The shortest interionic distances are 3.26 and 3.36 Å for F4···C3G and C3D···C3F, respectively, and the shortest distances between ions and the ether solvate are 3.68 and 3.75 Å for CS1···F2 and CS3···C3D, respectively. Distances and angles for **1**, $n = 4$, are presented in Table IV, and an ORTEP drawing of the coordination core with selected distances and angles is shown in Figure 5. The geometry of the cation can be described as square with a significant tetrahedral distortion due to steric crowding. Thus the angles at the metal atom between trans ligands, which would be 180° in a square-planar situation, are 150.13 (7) and 155.61 (7)°. The distortion from square planar is best seen in the ORTEP stereoview shown in Figure 6. Another measure of the extent of this distortion is provided by the dihedral angles between planes formed by oppositely oriented Rh, P, P triangles. These angles. are 0 and 90°, respectively, for idealized square-planar and tetrahedral geometries. In **1**, $n = 4$, the angles are 39 and 37°. The distortion in $[Rh(dppb)_2]^+$ is nearly as great as that found in $[Rh(PMe_3)_4]^+$,[19] in which case these angles are both

(18) Chaloner, P., private communication.

(19) Jones, R. A.; Real, F. M.; Wilkinson, G.; Galas, A. M. R.; Hursthouse, M. B.; Malik, K. M. A. *J. Chem. Soc., Dalton Trans.* **1980**, 511.

Table III. Positional and Thermal Parameters and Their Estimated Standard Deviations for [Rh(cod)(dppb)]BF_4

atom	x	y	z	B, Å² [a]	atom	x	y	z	B, Å² [a]
Rh	0.14836 (1)	−0.03329 (4)	0.31471 (2)	2.009	C12	0.1864 (3)	0.2061 (7)	0.4032 (3)	5.891
P1	0.11737 (4)	−0.0134 (1)	0.20729 (5)	1.973	B	0.3703 (3)	−0.173 (1)	0.9597 (5)	7.873
P2	0.17883 (4)	−0.2425 (1)	0.31700 (5)	2.175	H2A	0.0139 (0)	0.1009 (0)	0.1225 (0)	5.0000 (0)
F1	0.3701 (3)	−0.1465 (7)	0.9066 (2)	12.086	H3A	−0.0169 (0)	0.3043 (0)	0.0743 (0)	5.7000 (0)
F2	0.3902 (2)	−0.2921 (6)	0.9704 (3)	8.003	H4A	0.0396 (0)	0.4690 (0)	0.0913 (0)	6.0000 (0)
F3	0.4038 (2)	−0.0830 (6)	1.0003 (3)	12.225	H5A	0.1280 (0)	0.4339 (0)	0.1550 (0)	4.3000 (0)
F4	0.3278 (2)	−0.1594 (11)	0.9461 (4)	18.030	H6A	0.1627 (0)	0.2328 (0)	0.2085 (0)	3.7000 (0)
C1	0.1627 (2)	−0.0471 (6)	0.1816 (2)	2.345	H2B	0.0485 (0)	−0.1386 (0)	0.2338 (0)	3.6000 (0)
C2	0.2156 (2)	−0.1014 (6)	0.2316 (2)	2.750	H3B	−0.0230 (0)	−0.2830 (0)	0.1775 (0)	4.7000 (0)
C3	0.2171 (2)	−0.2490 (6)	0.2376 (2)	3.090	H4B	−0.0518 (0)	−0.3502 (0)	0.0751 (0)	5.2000 (0)
C4	0.1768 (2)	−0.3066 (5)	0.2470 (2)	2.765	H5B	−0.0129 (0)	−0.2718 (0)	0.0243 (0)	5.9000 (0)
C1A	0.0907 (2)	0.1437 (5)	0.1691 (2)	2.043	H6B	0.0574 (0)	−0.1226 (0)	0.0773 (0)	4.9000 (0)
C2A	0.0383 (2)	0.1686 (6)	0.1303 (2)	3.654	H2C	0.0924 (0)	−0.4173 (0)	0.2360 (0)	4.2000 (0)
C3A	0.0207 (2)	0.2903 (7)	0.1023 (3)	4.988	H3C	0.0446 (0)	−0.5651 (0)	0.2585 (0)	4.4000 (0)
C4A	0.0532 (3)	0.3851 (7)	0.1117 (3)	4.781	H4C	0.0665 (0)	−0.5938 (0)	0.3636 (0)	4.0000 (0)
C5A	0.1057 (3)	0.3634 (6)	0.1500 (3)	3.236	H5C	0.1387 (0)	−0.4895 (0)	0.4488 (0)	3.2000 (0)
C6A	0.1255 (2)	0.2444 (6)	0.1797 (2)	2.797	H6C	0.1866 (0)	−0.3463 (0)	0.4283 (0)	3.2000 (0)
C1B	0.0615 (2)	−0.1211 (5)	0.1619 (2)	2.236	H2D	0.2372 (0)	−0.4764 (0)	0.3782 (0)	4.2000 (0)
C2B	0.0365 (2)	−0.1660 (6)	0.1905 (2)	2.988	H3D	0.3276 (0)	−0.5251 (0)	0.4462 (0)	5.3000 (0)
C3B	−0.0064 (2)	−0.2501 (6)	0.1579 (2)	3.715	H4D	0.3894 (0)	−0.3536 (0)	0.4850 (0)	5.9000 (0)
C4B	−0.0234 (2)	−0.2889 (6)	0.0972 (3)	4.523	H5D	0.3629 (0)	−0.1404 (0)	0.4604 (0)	5.8000 (0)
C5B	0.0008 (2)	−0.2442 (7)	0.0680 (3)	5.157	H6D	0.2733 (0)	−0.0893 (0)	0.3937 (0)	4.9000 (0)
C6B	0.0424 (2)	−0.1589 (6)	0.0996 (2)	3.478	H1′	0.1666 (0)	0.0313 (0)	0.1640 (0)	3.5000 (0)
C1C	0.1429 (2)	−0.3658 (5)	0.3308 (2)	2.157	H1	0.1454 (0)	−0.1092 (0)	0.1465 (0)	3.5000 (0)
C2C	0.1021 (2)	−0.4316 (5)	0.2799 (3)	3.107	H2′	0.2263 (0)	−0.0646 (0)	0.2725 (0)	4.0000 (0)
C3C	0.0735 (2)	−0.5181 (6)	0.2926 (4)	4.695	H2	0.2410 (0)	−0.0743 (0)	0.2225 (0)	4.0000 (0)
C4C	0.0866 (2)	−0.5372 (6)	0.3544 (3)	2.683	H3′	0.2507 (0)	−0.2741 (0)	0.2730 (0)	4.0000 (0)
C5C	0.1281 (2)	−0.4751 (6)	0.4032 (3)	2.177	H3	0.2126 (0)	−0.2837 (0)	0.1994 (0)	4.0000 (0)
C6C	0.1561 (2)	−0.3897 (6)	0.3925 (2)	2.411	H4′	0.1806 (0)	−0.3992 (0)	0.2508 (0)	3.5000 (0)
C1D	0.2467 (2)	−0.2783 (6)	0.3785 (2)	2.807	H4	0.1422 (0)	−0.2898 (0)	0.2090 (0)	3.5000 (0)
C2D	0.2632 (2)	−0.4055 (6)	0.3948 (2)	3.116	H5	0.1626 (0)	0.1864 (0)	0.3062 (0)	4.0000 (0)
C3D	0.3157 (2)	−0.4344 (6)	0.4348 (2)	4.038	H6	0.0807 (0)	0.1262 (0)	0.2590 (0)	3.5000 (0)
C4D	0.3521 (2)	−0.3365 (8)	0.4577 (3)	5.013	H7	0.0392 (0)	0.0518 (0)	0.3061 (0)	5.0000 (0)
C5D	0.3366 (2)	−0.2112 (7)	0.4433 (3)	5.039	H7′	0.0579 (0)	0.1803 (0)	0.3445 (0)	5.0000 (0)
C6D	0.2836 (2)	−0.1801 (6)	0.4034 (2)	3.595	H8	0.0778 (0)	−0.0218 (0)	0.4029 (0)	4.0000 (0)
C5	0.1491 (2)	0.1774 (5)	0.3329 (2)	2.914	H8′	0.1197 (0)	0.0867 (0)	0.4306 (0)	4.0000 (0)
C6	0.1000 (2)	0.1364 (5)	0.3055 (2)	2.682	H9	0.1285 (0)	−0.1522 (0)	0.3819 (0)	3.7000 (0)
C7	0.0714 (2)	0.1032 (7)	0.3375 (3)	3.919	H10	0.2132 (0)	−0.1026 (0)	0.4240 (0)	3.5000 (0)
C8	0.1011 (2)	0.0260 (6)	0.3955 (2)	2.805	H11	0.2494 (0)	0.0991 (0)	0.4522 (0)	6.0000 (0)
C9	0.1409 (2)	−0.0647 (5)	0.3990 (2)	2.508	H11′	0.2204 (0)	0.1143 (0)	0.4867 (0)	6.0000 (0)
C10	0.1905 (2)	−0.0339 (6)	0.4221 (2)	3.195	H12	0.2099 (0)	0.2726 (0)	0.4081 (0)	7.5000 (0)
C11	0.2153 (2)	0.0985 (7)	0.4452 (2)	4.581	H12′	0.1652 (0)	0.2439 (0)	0.4179 (0)	7.5000 (0)

[a] Equivalent isotropic B's are reported here; anisotropic thermal parameters are reported in the supplementary material for all nonhydrogen atoms.

Table IV. Selected Distances and Angles in [Rh(dppb)$_2$]$BF_4 \cdot C_4H_{10}O$

Distances (Esd), Å

Rh-P1	2.324 (2)	P2-C13	1.878 (7)	P4-C33	1.871 (7)
Rh-P2	2.304 (2)	P2-C1C	1.824 (7)	P4-1G	1.840 (7)
Rh-P3	2.327 (2)	P2-C1D	1.845 (6)	P4-1H	1.822 (7)
Rh-P4	2.361 (2)	P3-C30	1.870 (7)	C11-C12	1.57 (1)
P1-C10	1.869 (7)	P3-C1E	1.830 (7)	C12-C13	1.56 (1)
P1-C1A	1.862 (7)	P3-C1F	1.833 (7)	C30-C31	1.59 (1)
P1-C1B	1.812 (7)	C10-C11	1.56 (1)	C31-C32	1.50 (1)
B-F1	1.34 (2)	B-F2	1.40 (2)	C32-C33	1.55 (1)
B-F3	1.23 (2)	B-F4	1.23 (2)		

Angles (Esd), Deg

P1-Rh-P2	90.97 (7)	Rh-P2-C13	110.2 (2)	C1A-P1-C1B	101.7 (3)
P1-Rh-P3	155.61 (7)	Rh-P2-C1C	114.0 (2)	C1C-P2-C1D	102.4 (3)
P1-Rh-P4	96.10 (6)	Rh-P2-C1D	125.9 (2)	C1E-P3-C1F	96.2 (3)
P2-Rh-P3	95.92 (7)	Rh-P3-C30	118.7 (2)	C1G-P4-C1H	106.7 (3)
P2-Rh-P4	150.13 (7)	Rh-P3-C1E	121.9 (2)	F1-B-F2	99 (1)
P3-Rh-P4	89.50 (6)	Rh-P3-C1F	108.4 (2)	F1-B-F3	114 (2)
Rh-P1-C10	122.9 (2)	Rh-P4-C33	120.3 (2)	F1-B-F4	118 (2)
Rh-P1-C1A	125.1 (2)	Rh-P4-C1G	120.6 (2)	F2-B-F3	91 (2)
Rh-P1-C1B	104.7 (2)	Rh-P4-C1H	116.6 (2)	F2-B-F4	111 (2)
				F3-B-F4	116 (2)

42°. It is evident that this distortion from the unexpected square-planar geometry is due to intramolecular phosphine–phosphine repulsions. The shortest intramolecular interphosphine distances are 2.29 Å for H6D···H6E and 3.37 and 3.65 Å for C1C···C1E and C1A···C1G, respectively. Examination of a model constructed from the atomic coordinates shows that the latter C···C distances would become unacceptably short as the geometry is distorted to square planar. Indeed, 3.37 Å is already short for an aromatic C···C distance.[20] It is interesting to note the effect these repulsions

Table V. Selected Distances and Angles in $[Rh(cod)(dppb)]BF_4$

		Distances (Esd), Å			
Rh-P1	2.317 (2)	P2-C4	1.843 (6)	C7-C8	1.46 (1)
Rh-P2	2.342 (2)	P2-C1C	1.838 (6)	C8-C9	1.504 (9)
Rh-C5	2.221 (6)	P2-C1D	1.823 (6)	C10-C11	1.52 (1)
Rh-C6	2.225 (6)	C1-C2	1.511 (9)	C11-C12	1.45 (1)
Rh-C9	2.267 (6)	C2-C3	1.530 (9)	C12-C5	1.51 (1)
Rh-C10	2.254 (6)	C3-C4	1.501 (9)	B-F1	1.35 (2)
P1-C1	1.859 (6)	C5-C6	1.336 (9)	B-F2	1.33 (2)
P1-C1A	1.832 (6)	C9-C10	1.334 (9)	B-F3	1.35 (2)
P1-C1B	1.824 (6)	C6-C7	1.52 (1)	B-F4	1.16 (2)
		Angles (Esd), Deg			
P1-Rh-P2	90.78 (6)	C5-Rh-C6	35.0 (2)	Rh-P2-C4	120.3 (2)
P1-Rh-C5	95.9 (1)	C9-Rh-C10	34.3 (2)	Rh-P2-C1C	118.8 (2)
P1-Rh-C6	89.2 (1)	C5-Rh-C9	86.8 (2)	Rh-P2-C1D	117.6 (2)
P1-Rh-C9	155.0 (1)	C5-Rh-C10	79.8 (2)	C1A-P1-C1B	102.6 (3)
P1-Rh-C10	170.2 (1)	C6-Rh-C9	78.8 (2)	C1C-P2-C1D	103.1 (3)
P2-Rh-C5	160.0 (2)	C6-Rh-C10	92.2 (2)	C1-P1-C1A	100.9 (3)
P2-Rh-C6	164.5 (1)	Rh-P1-C1	118.6 (2)	C1-P1-C1B	107.2 (3)
P2-Rh-C9	95.1 (1)	Rh-P1-C1A	117.7 (2)	C4-P2-C1C	102.8 (3)
P2-Rh-C10	90.5 (1)	Rh-P1-C1B	108.2 (2)	C4-P2-C1D	98.9 (3)
Rh-C5-C6	72.7 (4)	Rh-C9-C10	72.3 (4)	C11-C12-C5	117.7 (6)
Rh-C6-C5	72.3 (4)	Rh-C10-C9	73.4 (4)	C7-C8-C9	116.1 (6)
Rh-C5-C12	110.3 (4)	Rh-C9-C8	110.6 (5)	F1-B-F2	98 (1)
Rh-C6-C7	108.3 (4)	Rh-C10-C11	107.0 (5)	F1-B-F3	101 (1)
C6-C5-C12	125.5 (7)	C8-C9-C10	124.9 (6)	F1-B-F4	107 (1)
C5-C6-C7	128.1 (7)	C9-C10-C11	126.4 (6)	F2-B-F3	114 (1)
C6-C7-C8	115.1 (6)	C10-C11-C12	115.9 (6)	F2-B-F4	119 (1)
				F3-B-F4	114 (1)

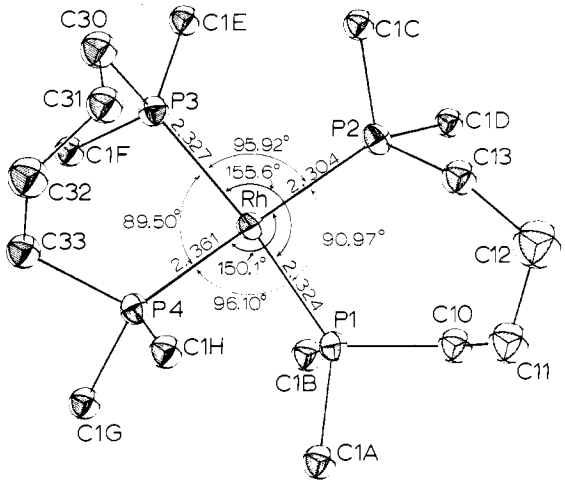

Figure 5. ORTEP drawing of the coordination core of $[Rh(dppb)_2]^+$ with selected distances and angles.

have on the geometry of the diphosphine ligands themselves. The Rh–P–C angles are significantly greater than tetrahedral, averaging 117° and ranging from 105 to 126°. The P–Rh–P bite angles are 90.97 (7) and 89.50 (6)° and are compressed relative to the value of 97.56 (4)° found in $[Rh_2(CO)_4(dppb)_3](PF_6)_2$.[10]

The Rh–P distances show a significant variation, which is presumably due to phosphine–phosphine repulsions. The Rh–P4 distance is unusually long, 2.361 (2) Å, while its trans Rh–P2 distance is short, 2.304 (2) Å, relative to the other mutually trans distances, which are 2.327 (2) and 2.324 (2) Å. These distances are long compared with those found in $[Rh(dppe)_2]ClO_4$,[21] averaging 2.306 Å and ranging from 2.289 (6) to 2.313 (6) Å. Other distances and angles within the cation are normal.

The structure of **2** consists of discrete cations and anions. The shortest interionic distances are 2.40 and 2.43 Å for F3···H3A and H3′···H6A, respectively. Distances and angles for **2** are presented in Table V, and an ORTEP stereoview is shown in Figure 7. The coordination core geometry, which is defined by Rh, P1, and P2 and by the midpoints of the diolefin double bonds (C56 and C910), is best described as slightly distorted square planar. Thus the angles at the metal atom between trans ligands are 172 and 176° for P1–Rh–C910 and P2–Rh–C56, respectively, and the dihedral angles between the oppositely oriented planes (Rh, P1, P2—Rh, C56, C910 and Rh, P1, C56—Rh, P2, C910) are 7.7 and 7.5°, respectively. Note that this distortion is considerably less than for **1**, $n = 4$. In **2**, the less sterically demanding cod ligand does not cause the severe ligand–ligand repulsions which are operative in **1**, $n = 4$ (vide infra), and therefore this complex adopts the preferred planar coordination geometry. The Rh–P distances show some variation [2.317 (2) and 2.343 (2) Å for P1 and P2, respectively], and interestingly the Rh–C bonds reflect this difference such that the longer Rh–C bonds are trans to the shorter Rh–P bond [2.261 (6) and 2.223 (6) Å average for Rh–C5 and –C6 and Rh–C9 and –C10, respectively]. The average Rh–P distance [2.330 (2) Å] in **2** is identical with the average Rh–P distance in **1**, $n = 4$ [2.329 (2) Å], and both are somewhat longer than found in **1**, $n = 2$ [2.306 (6) Å].[21] The P–Rh–P bite angle in **2** [90.78 (6)] is similar to the average value found in **1**, $n = 4$ [90.24 (7)°].

The cod ligand takes its customary "tub" conformation with the olefin bonds oriented approximately normal to the coordination plane. The distances between rhodium and the double-bond centers of cod are 2.161 (6) and 2.119 (6) Å and are on the long end of the range 2.00–2.14 Å found in heavy-metal complexes with cod.[22-25] This lengthening probably results from the trans influence of the phosphine ligands. The coordinated double bonds, C5–C6 and C9–C10, have lengths of 1.336 (9) and 1.334 (9) Å, respectively, compared to an uncoordinated olefinic distance of 1.34 Å.[22] The

(20) Pauling, L. "The Nature of the Chemical Bond"; Cornell University Press: Ithaca, NY, 1960; pp 260–262.
(21) Hall, M. C.; Kilbourn, B. T.; Taylor, K. A. *J. Chem. Soc. A* **1970**, 2539.
(22) Churchill, M. R.; Bezman, S. A. *Inorg. Chem.* **1973**, *12*, 53 and references cited therein.
(23) Ibers, J. A.; Snyder, R. G. *Acta Crystallogr.* **1962**, *15*, 923.
(24) Coetzer, J.; Gafner, G. *Acta Crystallogr., Sect. B* **1970**, *B26*, 985.
(25) Kaiser, S. W.; Saillant, R. B.; Butler, W. M.; Rasmussen, P. G. *Inorg. Chem.* **1976**, *15*, 2681.

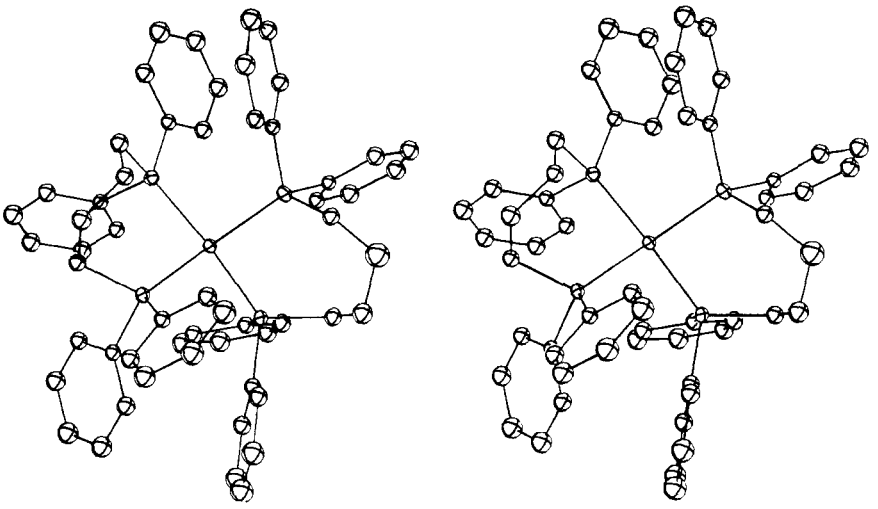

Figure 6. ORTEP stereoview of $[Rh(dppb)_2]^+$.

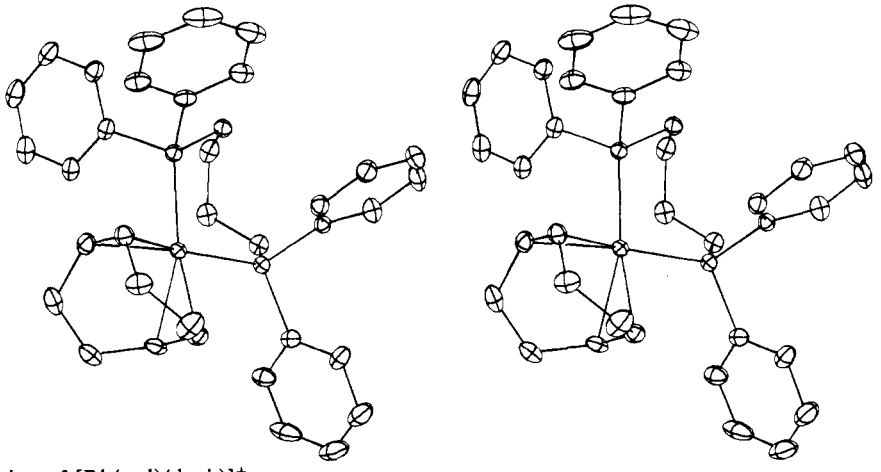

Figure 7. ORTEP stereoview of $[Rh(cod)(dppb)]^+$.

average coordinated olefin bond length of cod in $[Rh(cod)Cl]_2$ is 1.44 (7) Å.[23] The similarity of these bond lengths in **2** with those in uncoordinated cod is consistent with the long Rh–C bonds, which indicate weak bonding of the cod ligand. Carbon–carbon single-bond distances range from 1.45 (1) to 1.52 (1) Å, results typical for cod bonded to a heavy metal.[22]

Conclusions

Within the series of cationic bis(diphosphino) complexes of Rh(I), **1**, n = 2–4, low-temperature ^{31}P NMR data indicate that their solution geometries are the expected square planar for n = 2, solvated pentagonal bipyramidal for n = 3, and solvated and probably polynuclear for n = 4. Solid-state structural data are consistent with these observations. Thus the n = 2 complex is square planar[21] while the n = 4 complex is significantly distorted toward tetrahedral due to phosphine–phosphine repulsions. The latter complex also shows one lengthened Rh–P bond due to these repulsions, which is likely to result in the formation of dppb-bridged dimers. In **2** these repulsions are relieved, and the complex adopts a nearly square-planar geometry. It is clear from these observations that ligand–ligand repulsions in diphosphine complexes play a major role in determining geometry and reactivity. Indeed, the complexes **1**, n = 1–4, show a marked dependence on n for the rate of catalytic decarbonylation.[5,8] Also, the reaction of these complexes with CO illustrates a major reactivity difference. Simple monocarbonyl adducts $[Rh(diphosphine)_2CO]^+$ are isolated for n = 1 and 3,[16,17] no CO adduct is formed for n = 2, and the binuclear dppb-bridged complex $[Rh_2(dppb)_3(CO)_4]^{2+}$ is isolated for n = 4.[10]

Acknowledgment. Support of this research through a grant from the National Science Foundation is gratefully acknowledged (NSF No. CHE 78-21840). We also thank the NSF for partial support for our X-ray diffraction and structure-solving equipment (NSF Grant No. CHE 77-28505). The Johnson-Matthey Co. is gratefully acknowledged for a generous loan of $RhCl_3 \cdot H_2O$. M.P.A. is a participant in the U.S. Air Force Institute of Technology Graduate School Program.

Registry No. **1**, n = 3, 70196-21-3; **1**, n = 4, 79255-70-2; **2**, 79255-71-3; $[Rh(cod)Cl]_2$, 12092-47-6.

Supplementary Material Available: Tables of general temperature factor expressions, weighted least-squares planes, and calculated and observed structure factor amplitudes (37 pages). Ordering information is given on any current masthead page.